Wang-Landau sampling: Improving accuracy

A. A. Caparica[1] and A. G. Cunha-Netto[2]

[1]*Instituto de Física, Universidade Federal de Goiás, C.P. 131, CEP 74001-970 Goiânia, GO, Brazil*

[2]*Departamento de Física, Instituto de Ciências Exatas, and National Institute of Science and Technology for Complex Systems, Universidade Federal de Minas Gerais, C.P. 702, 30123-970 Belo Horizonte, Minas Gerais, Brazil*

(Received 16 September 2011; revised manuscript received 19 December 2011; published 5 April 2012)

In this work, we investigate the behavior of the microcanonical and canonical averages of the two-dimensional Ising model during the Wang-Landau simulation. The simulations were carried out using conventional Wang-Landau sampling and the $1/t$ scheme. Our findings reveal that the microcanonical average should not be accumulated during the initial modification factors f, and they outline a criterion to find this limit, which we define as f_{micro}. We show that updating the density of states only after every L^2 spin-flip trials leads to a much better precision. We present a mechanism to determine for the given model up to what final modification factor f_{final} the simulations should be carried out. Altogether these small adjustments lead to an improved procedure for simulations with much more reliable results. We compare our results with $1/t$ simulations. We also present an application of the procedure to a self-avoiding homopolymer.

DOI: 10.1103/PhysRevE.85.046702 PACS number(s): 02.70.−c

I. INTRODUCTION

In recent years, Wang-Landau sampling (WLS) [1,2] has been applied to many systems and has become a well-established Monte Carlo algorithm. The heuristic idea of the method is based on the fact that if one performs a random walk in energy space with a probability proportional to the reciprocal of the density of states, a flat histogram is generated for the energy distribution. Since the density of states produces huge numbers, instead of estimating $g(E)$, the simulation is performed for $S(E) \equiv \ln g(E)$, and a histogram $H(E)$ is accumulated during the simulations to control the frequency of visits to the energy levels. At the beginning of the simulation, we set $S(E) = 0$ for all energy levels. The random walk in the energy space runs through all energy levels from $E_{\min}$ to $E_{\max}$ with a probability

$$p(E \to E') = \min(\exp[S(E) - S(E')], 1), \tag{1}$$

where E and E' are the energies of the current and the new possible configurations. Whenever a configuration is accepted, we update $H(E') \to H(E') + 1$ and $S(E') \to S(E') + F$, where $F = \ln f$ (f is the so-called modification factor). The initial modification factor is taken as $f = f_0 = e = 2.718\,28\ldots$. If the trial configuration is not accepted, then the currents $H(E)$ and $S(E)$ are updated again. The flatness of the histogram is checked after a number of Monte Carlo (MC) steps, and usually the histogram is considered flat if $H(E) > 0.8\langle H\rangle$ for all energies, where $\langle H\rangle$ is an average over the energies. If the flatness condition is fulfilled, we update the modification factor to a finer one by setting $f_{i+1} = \sqrt{f_i}$ and reset the histogram $H(E) = 0$. Simulations are in general halted when $\ln f \sim 10^{-8}$. Having in hand the density of states, one can calculate the canonical average of any thermodynamic variable as

$$\langle X\rangle_T = \frac{\sum_E \langle X\rangle_E g(E) e^{-\beta E}}{\sum_E g(E) e^{-\beta E}}, \tag{2}$$

where $\langle X\rangle_E$ is the microcanonical average accumulated during the simulations and $\beta = 1/k_B T$, k_B is the Boltzmann constant, and T is the temperature. One of the interesting features of the method is that it can also access some quantities, such as the free energy and entropy, which are not directly available from conventional Monte Carlo simulations.

As described above, the convergence of the method depends on both the flatness criterion and the final f when the simulation is interrupted, but the best choice of each is not obvious for each model to be studied.

Recently, some authors have asserted that although achieving a flat histogram is the initial motivation of the WLS, the flatness is not a necessary criterion to reach convergence [3–6]. They argue that in the conventional WLS, the error saturates to a constant, while if $\ln f$ decreases as $1/t$, where t is a normalized Monte Carlo time, the error would decrease monotonically as well. The $1/t$ algorithm is divided into two steps. Initially the conventional WLS is followed, starting from $S(E) = 0$ and then constructing $S(E)$ using a histogram updated in every new accepted configuration. $S(E)$ is updated as in the conventional WLS, $S(E) = S(E) + F_i$, with the initial value $F_0 = 1$. After a number of moves (e.g., 1000 MC sweeps), we check $H(E)$ to verify whether all the levels were visited by the random walker at least once and then update $F_i = F_i/2$ and reset $H(E) = 0$. (The flatness criterion is not required, even in this first stage.) Simulation is performed while $F_i \geqslant 1/t = N/j$, where j is the number of trial moves and N is the number of energy levels. In the remainder of the simulation, F_i is updated every new configuration as $F_i = 1/t$ up to a final chosen precision F_{final}.

The efficiency, convergence, and limitations of the WLS have been quantitatively studied [7,8]. In the present work, we perform a practical, computational study on the convergence and the accuracy of the method.

In this paper, we investigate the behavior of the maxima of the specific heat,

$$C = \langle\!\langle (E - \langle E\rangle)^2\rangle\!\rangle / T^2, \tag{3}$$

and the susceptibility,

$$\chi = L^2 \langle\!\langle (m - \langle |m|\rangle)^2\rangle\!\rangle / T, \tag{4}$$

where E is the energy of the configurations and m is the corresponding magnetization per spin during the conventional WLS and the $1/t$ algorithm simulations for the Ising model on a square lattice [9]. We observe (as in [4–6,10]) that a considerable part of the conventional Wang-Landau simulation is not very useful because the error saturates. We propose some strategies to improve the efficiency of the WLS and compare our results with exact calculations [11]. Our findings lead to a new way of performing the WLS simulations.

II. A NEW PROCEDURE FOR SIMULATIONS

In order to test how far the simulations should go, during the WLS, beginning from f_{17}, we calculate the specific heat and the susceptibility defined in Eqs. (3) and (4), as well as the energy and the magnetization at some fixed temperatures. We use the current $g(E)$, and from this time on these mean values are updated whenever we check the flatness of the histogram. Figure 1 shows the evolution of the temperature of the maximum of the specific heat calculated for $L = 32$ for eight independent runs as a function of the Monte Carlo sweeps (MCS) [12] and compares these results with the value obtained using the exact data of Ref. [11] [$T_c(L = 32) = 2.293\,929\,79$]. The dots label the MCS when the modification factor was updated, the leftmost in each run corresponding to f_{17}. One can see that around $\ln f_{23} = 1.1921 \times 10^{-7}$, all the curves become stabilized in values displaced close to the exact value. Any further computational effort for $\ln f < \ln f_{23}$ does not lead to a better convergence.

In order to investigate how these results are displaced around the exact value, we performed 100 000 independent runs of WLS for $L = 8$ using the 80%- and the 90%-flatness criteria and built up histograms using bins of width 0.001. In Fig. 2, we show that the histograms form nice Gaussians centered close, but not precisely in the exact value. In Fig. 3, we show the same evolution for the temperature of the maximum of the susceptibility. One can see that in this case the curves do not flow to steady values.

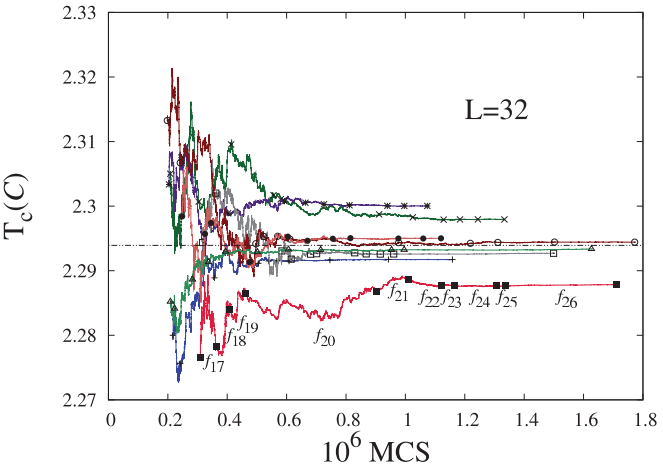

FIG. 1. (Color online) Evolution of the temperature of the extremum of the specific heat during the WLS, beginning from f_{17}, for eight independent runs using the 80%-flatness criterion. The dots show where the modification factors were updated and the straight line is the result obtained using the exact data from Ref. [11].

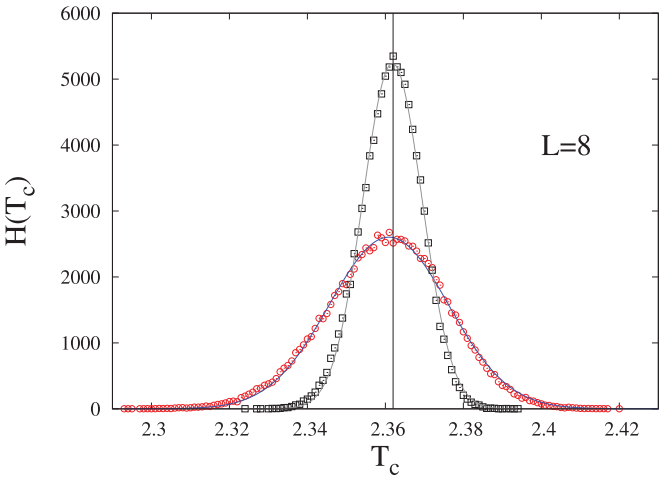

FIG. 2. (Color online) Histograms of the locations of the peak of the specific heat for the 2D Ising model during the WLS, using the 80%- and 90%-flatness criteria, each for 100 000 independent runs, along with their best-fit Gaussians. The central line corresponds to the exact temperature of the maximum of the specific heat obtained with data from Ref. [11].

A strategy to improve the precision of the WLS is to update the density of states periodically (i.e., after every p trial configuration), instead of updating $S(E)$ every spin-flip trial. In order to investigate how this change affects the final result, we performed 100 000 independent runs ($L = 8$) using the 80%-flatness criterion and constructed again histograms of the locations of the peak of the specific heat. We tested the WLS with different values for p. Figure 4 shows the Gaussian best fits for $p = 1$ (conventional WLS), $p = L$, and $p = L^2$. The vertical line indicates the exact value using Ref. [11]. One can see that the higher the values of p, the narrower are the Gaussian curves. Defining the relative error $\varepsilon(X)$ for any

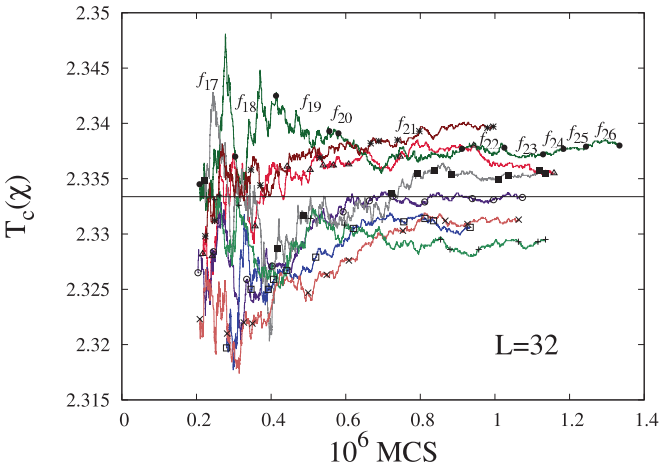

FIG. 3. (Color online) Evolution of the temperature of the extremum of the susceptibility during the WLS, beginning from f_{17}, for eight independent runs using the 80%-flatness criterion. The dots show where the modification factors were updated and the straight line is the result obtained using the exact data from Ref. [11].

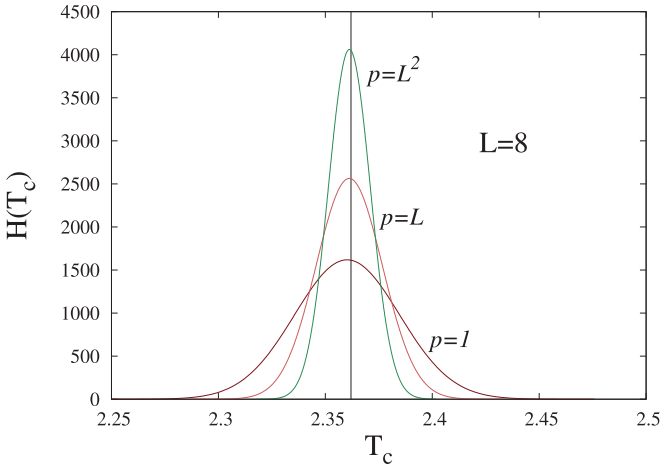

FIG. 4. (Color online) Best-fit Gaussians for the histograms of the temperatures of the peak of the specific heat for the 2D Ising model during the WLS up to $\ln f = 10^{-4}$, using the 80%-flatness criterion, each for 100 000 independent runs with the density of states being updated every p spin-flip trial. The central line corresponds to the exact temperature obtained with data from Ref. [11].

quantity X by

$$\varepsilon(X) = \frac{|X_{\text{sim}} - X_{\text{exact}}|}{X_{\text{exact}}}, \tag{5}$$

we obtain the relative errors of the simulated mean values with respect to the result using Ref. [11] for $p = 1$, L, and L^2 as 0.000 43, 0.000 19, and 0.000 13, respectively. These results suggest that one would obtain even higher accuracy for $p > L^2$, but the consumption of CPU time would be prohibitive. Therefore, one should update the density of states only after L^2 trial moves since it leads to more accurate results [13,14]. In other words, adopting the Monte Carlo step (L^2 trial moves), as is conventional in the METROPOLIS algorithm, is also convenient in the Wang-Landau algorithm.

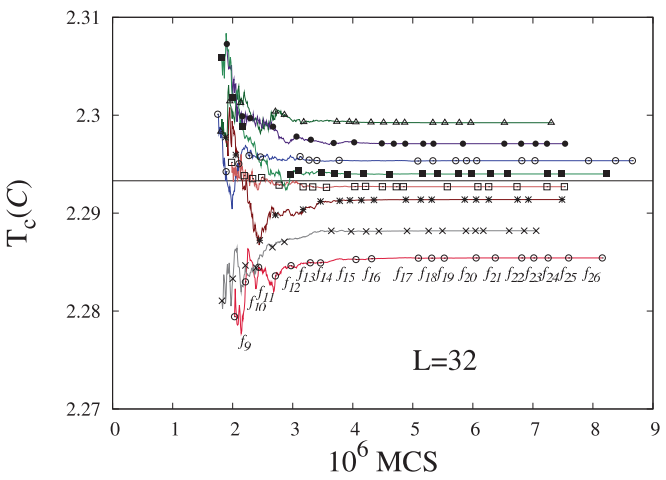

FIG. 5. (Color online) Evolution of the temperature of the extremum of the specific heat during the WLS, beginning from f_9, for eight independent runs. The density of states was updated after every L^2 trial move and the flatness criterion was 80%. The dots show where the modification factor was updated and the straight line is the result obtained using the exact data from Ref. [11].

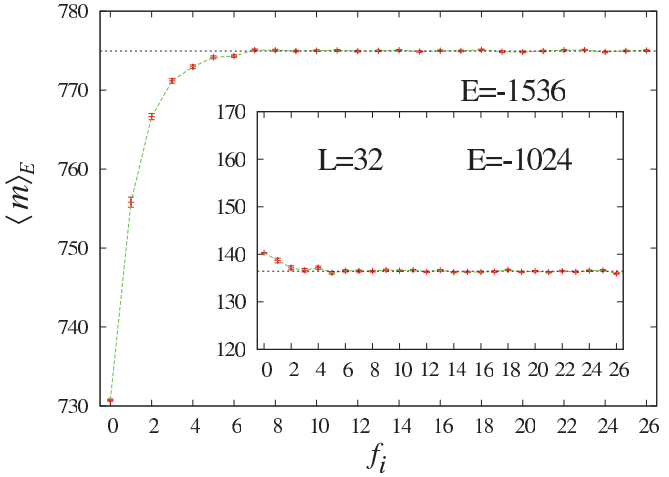

FIG. 6. (Color online) Evolution of the microcanonical average of the magnetization for the 2D Ising model for $L = 32$ at $E = -1024$ and -1536 during the simulations over 1000 independent runs for each flatness stage.

In Fig. 5, we show the evolution of the location of the maximum of the heat capacity during WLS in which the density of states was updated only after every L^2 spin-flip trial, beginning from f_9. We see that now the curves flow to steady values around $\ln f = \ln f_{13} = 1.2208 \times 10^{-4}$ and simulations with higher orders of the modification factor are unnecessary. One can see that if the simulations adopting the Monte Carlo step become longer, the canonical averages converge to constant values much earlier.

Before investigating the behavior of the peak of the susceptibility during the simulations, we turn our attention to another important detail. What is the behavior of the microcanonical averages $\langle M \rangle_E$ and $\langle M^2 \rangle_E$ during the sampling process? We have also evaluated the microcanonical averages during the simulations. In order to estimate the mean value of the

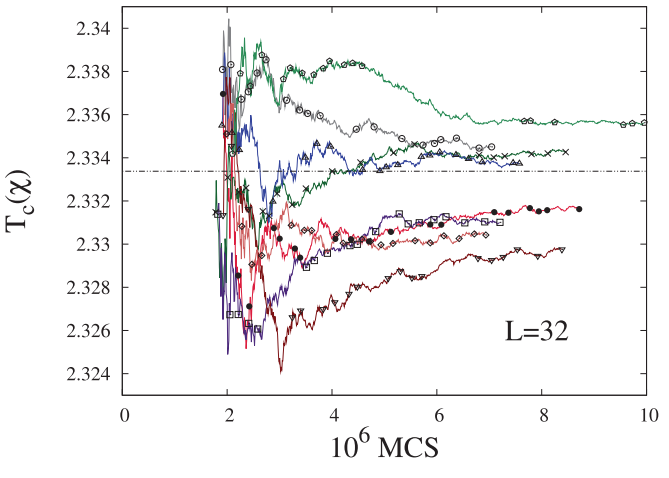

FIG. 7. (Color online) Evolution of the temperature of the extremum of the susceptibility during the WLS, beginning from f_9, for eight independent runs. The density of states was updated after every L^2 trial move and the flatness criterion was 80%. The dots show where the modification factor was updated and the straight line is the result obtained using the exact data from Ref. [11] with the microcanonical average accumulated from $\ln f = \ln f_7$.

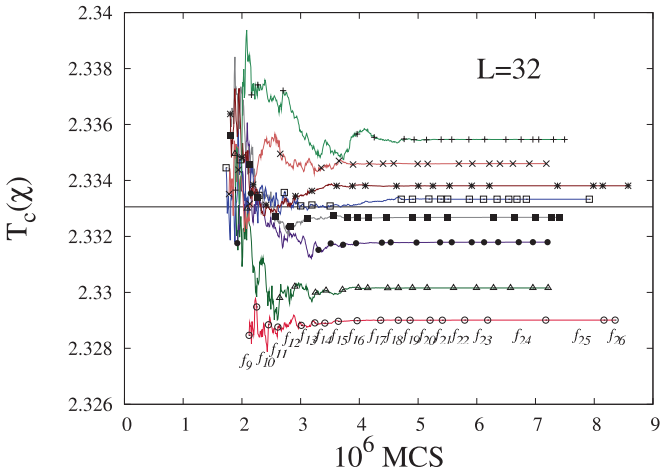

FIG. 8. (Color online) Evolution of the temperature of the extremum of the susceptibility during the WLS, beginning from f_9, for eight independent runs, using a common microcanonical average in 24 independent runs. The density of states was updated after every L^2 trial move and the flatness criterion was 80%. The dots show where the modification factor was updated and the straight line is the result obtained using the exact data from Ref. [11] with the microcanonical average accumulated from $\ln f = \ln f_7$.

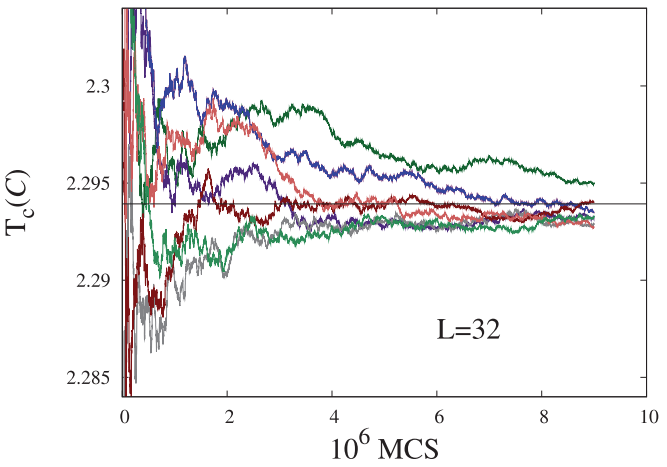

FIG. 9. (Color online) Evolution of the temperature of the extremum of the specific heat during the $1/t$ simulations for eight independent runs beginning from the second stage. The straight line is the result obtained using the exact data from Ref. [11]. Simulations were halted when the CPU time matched the mean time of WLS.

magnetization during each flatness stage, we carried out 1000 independent runs and calculated $\langle M\rangle_E$ for each f_i with $i = 0,1,2,\ldots,26$. In Fig. 6, we show these results for two energy levels and see that they flow to relatively stable values around $f_{\text{micro}} = f_7$. We therefore conclude that the microcanonical averages should not be accumulated before $\ln f \leqslant \ln f_{\text{micro}} = \ln f_7 = 7.843 \times 10^{-3}$ for the 2D Ising model.

In Fig. 7, we show the evolution of the maximum of the susceptibility during the simulations beginning from f_9, updating the density of states after every L^2 spin-flip trial and accumulating the microcanonical averages only for $\ln f \leqslant \ln f_{\text{micro}} = \ln f_7$. We observe that even for $\ln f = \ln f_{26} \approx 10^{-8}$, we do not obtain stable values like those of Fig. 5. However, if one takes the mean value of the microcanonical averages in 24 independent runs and uses this result for calculating the canonical averages during the simulations, the averages do flow to stable values, as shown in Fig. 8. Since the mean values obtained from each independent run are well distinct from each other, one can define f_{final} on the very beginning of the straight line that occurs in each case. The results shown in Figs. 5 and 8 define, therefore, that the simulations should be continued only up to $f_{\text{final}} = f_{13}$ for the 2D Ising model. The evolution of the canonical averages of the energy and the magnetization at a given temperature yields evidently patterns similar to those of Figs. 5 and 8 with the same limit modification factors.

By applying the method to a new model, one should take a representative size and find out when the corresponding canonical averages obtained from a few independent runs would come to steady values, defining, therefore, f_{final} for the given model. We would like to stress that all modification factors defined above using the canonical and microcanonical averages during the simulations apply to the 2D Ising model, and it is important to perform studies similar to those of Figs. 5, 6, and 8 before adopting this new procedure to other models to be sure about where to halt the simulations and where to begin accumulating the microcanonical averages.

In view of the above observations, we propose the following new procedure for simulations:

(i) Instead of updating the density of states after every spin-flip, we ought to update it after each Monte Carlo sweep.

(ii) WLS should be carried out only up to $\ln f = \ln f_{\text{final}}$ defined by the canonical averages during the simulations.

(iii) The microcanonical averages should not be accumulated before $\ln f \leqslant \ln f_{\text{micro}}$ defined by the microcanonical averages during the simulation.

III. COMPARISON WITH $1/T$ SIMULATIONS

Figure 9 shows the evolution of the maxima of the specific heat during the simulations using the $1/t$ scheme, beginning from the second stage and halting the simulations when the CPU time matched up the mean time of the simulations of Fig. 5.

In order to compare these results, we performed 100 000 independent runs of WLS for $L = 8$ up to $\ln f_{\text{final}} = \ln f_{13}$ using 80%- and 90%-flatness criteria (WL.f_{13}.80% and WL.f_{13}.90%) and built up the histograms. Next we carried out similar simulations using the $1/t$ algorithm, halting the simulation when the CPU time matched up those of WL.f_{13} ($1/t_{80\%}$ and $1/t_{90\%}$). In Fig. 10, we show the best-fit Gaussians of the histograms. One can see that they are not really centered around the exact value. The relative errors of the simulated mean values with respect to the result using Ref. [11] yield 0.000 41 and 0.000 36, respectively, for WL.f_{13}.80% and WL.f_{13}.90%, and 0.0017 and 0.000 81 for $1/t_{80\%}$ and $1/t_{90\%}$, with final F_k reaching 5.1×10^{-7} and 2.4×10^{-7}. We see that although the widths of the $1/t$ curves are smaller, their centers are farther apart from the exact value than those of WLS, revealing a biased estimation effect in the $1/t$ method.

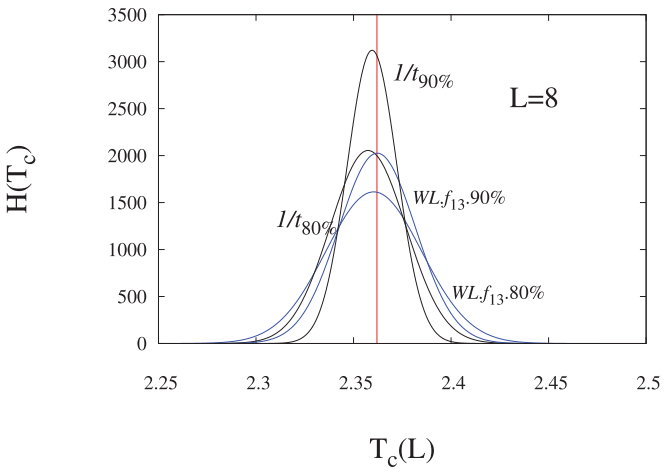

FIG. 10. (Color online) Best-fit Gaussians for the histograms of the temperatures of the peak of the specific heat for the 2D Ising model during the WLS up to $f_{\text{final}} = f_{13}$, using the 80%- and 90%-flatness criteria, each for 100 000 independent runs. The $1/t$ simulations were carried out within the same CPU time. The central line corresponds to the exact temperature obtained with data from Ref. [11].

IV. FINITE-SIZE SCALING

According to finite-size scaling theory [15–17] from the definition of the free energy one can obtain the zero-field scaling expressions for the magnetization and the susceptibility, respectively, by

$$m \approx L^{-\beta/\nu}\mathcal{M}(tL^{1/\nu}), \tag{6}$$

$$\chi \approx L^{\gamma/\nu}\mathcal{X}(tL^{1/\nu}). \tag{7}$$

We see that the locations of the maxima of these functions scale asymptotically as

$$T_c(L) \approx T_c + a_q L^{-1/\nu}, \tag{8}$$

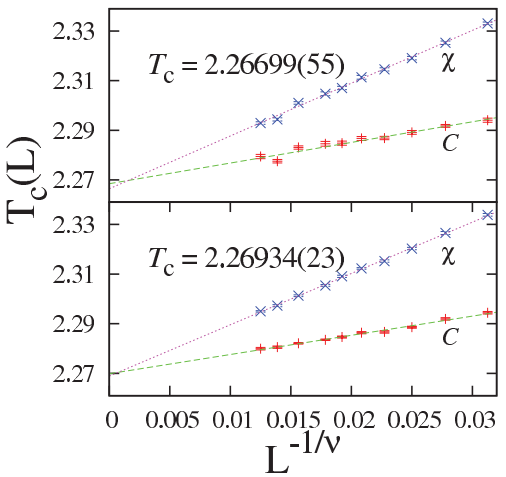

FIG. 11. (Color online) Size dependence of the locations of the extrema in the specific heat and the susceptibility for conventional WLS (top) and using our procedure (bottom) assuming $\nu = 1$.

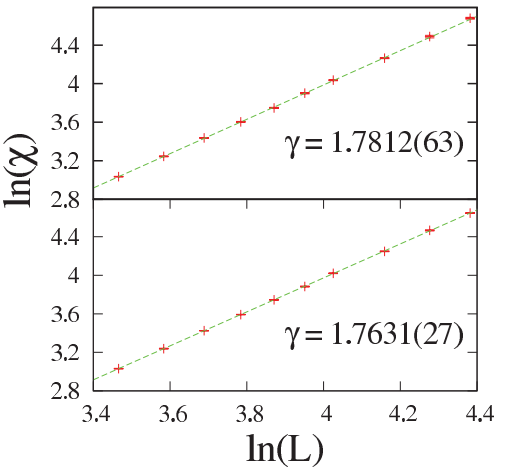

FIG. 12. (Color online) Log-log plot of the size dependence of the finite-lattice susceptibility at $T_c(L)$ with 80%-flatness criterion for conventional WLS (top) and using our procedure (bottom).

where a_q is a quantity-dependent constant, allowing then the determination of T_c.

In order to compare the efficiency of the conventional WLS, the $1/t$ scheme, and our procedure, we performed simulations with $L = 32$, 36, 40, 44, 48, 52, 56, 64, 72, and 80, taking $N = 24$, 24, 20, 20, 20, 16, 16, 16, 12, and 12 independent runs for each size, respectively.

Using these scaling functions, we estimated the critical temperature and the critical exponents β and γ. Taking a microcanonical average including all independent runs was important to reveal in Fig. 8 that for quantities that involve the magnetization, the simulations can also be carried out only up to $f_{\text{final}} = f_{13}$, but such a procedure does not lead to better results for the estimation of the canonical averages.

Assuming $\nu = 1$, we can use Eq. (11) to determine T_c as the extrapolation to $L \to \infty$ ($L^{-1/\nu} = 0$) of the linear fits given

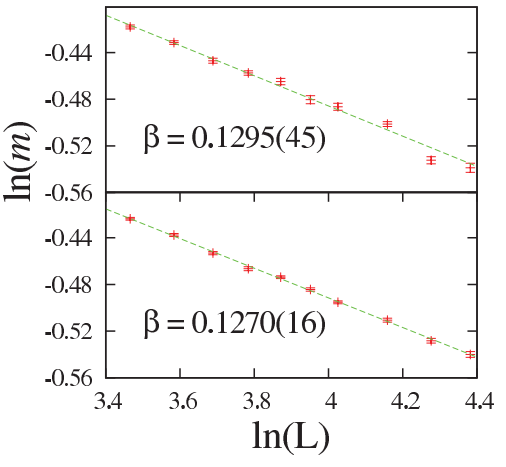

FIG. 13. (Color online) Log-log plot of the size dependence of the finite-lattice magnetization with 80%-flatness criterion for conventional WLS at $T_c = 2.266\,99$ (top) and using our procedure at $T_c = 2.269\,34$ (bottom).

TABLE I. Finite-size scaling results for the critical temperature and the critical exponents β and γ. The CPU times are expressed in terms of the time spent by the conventional WLS with 80% flatness.

Case	T_c	β	γ	CPU time
Exact	2.269 185 3 ...	0.125	1.75	
$1/t$				
1×10^{-6}	2.262 1(11)	0.197(14)	1.943(35)	0.15
5×10^{-7}	2.264 2(11)	0.147 9(84)	1.846(18)	0.30
1×10^{-7}	2.268 48(35)	0.129 7(31)	1.7833(46)	1.51
5×10^{-8}	2.269 04(25)	0.125 9(21)	1.7708(23)	3.03
1×10^{-8}	2.269 44(11)	0.126 47(94)	1.7616(17)	15.13
		Conventional WLS		
80%	2.266 99(55)	0.129 5(45)	1.7812(63)	1.00
90%	2.268 29(33)	0.138 6(51)	1.7899(87)	1.75
		Our procedure		
80%	2.269 34(23)	0.127 0(16)	1.7631(27)	9.78
90%	2.269 16(12)	0.124 94(68)	1.7555(32)	22.21

by the locations of the maxima of the specific heat and the susceptibility defined by Eqs. (3) and (4). In Fig. 11, we show the linear fits that converge to T_c at $L^{-1/\nu} = 0$ for conventional WLS and the new procedure, both using the 80%-flatness criterion. The final estimate for T_c was taken as the mean value obtained from both fits.

Since T_c is now estimated, we can calculate the critical exponents β and γ. According to Eq. (7), the maximum of the finite-lattice susceptibility defined by Eq. (4) is asymptotically proportional to $L^{\gamma/\nu}$. In Fig. 12, we show these results for the conventional WLS and our procedure, both using the 80% criterion of flatness. In the vicinity of the critical temperature, the magnetization scales as $L^{-\beta/\nu}$. We can use Eq. (6) at the critical point to calculate the exponent β directly from the slope of the log-log graph and find β. In Fig. 13, we show again the results for conventional WLS and our procedure for this exponent. One can see that in all cases our procedure is more accurate than the conventional WLS.

For the conventional WLS and the new procedure proposed here, simulations were carried out using 80%- and 90%-flatness criteria, and for the $1/t$ scheme the simulations were halted for $\ln f = 10^{-6}, 5 \times 10^{-7}, 10^{-7}, 5 \times 10^{-8}$, and 10^{-8}. In Table I, we show the results for the $1/t$ simulations, the conventional WLS, and our procedure along with the exact values. The $1/t$ results become accurate only when $\ln f \sim 5 \times 10^{-8}$, and for lower values of $\ln f$ they become worse, giving the impression that they are already fluctuating around the true value. The conventional WLS displays problems of accuracy, while our results are adequately accurate for both 80%- and 90%-flatness criteria. It is worth mentioning that we have obtained high-resolution values using the 90%-flatness criterion, which should be compared with the erratic behavior of the $1/t$ simulations for $\ln f < 5 \times 10^{-8}$, but such a stringent level of flatness is difficult to apply to other systems [14,18–20], resulting sometimes in nonconvergence or even more inaccurate values. Moreover, the 90%-flatness criterion simulations are very time consuming. We conclude, therefore, that the widely adopted 80%-flatness criterion is indeed the best guess, since it is applicable to all systems.

V. APPLICATION TO A SELF-AVOIDING HOMOPOLYMER

In this section, we apply to a homopolymer the initial tests to determine up to which modification factor f_{final} one should continue the WLS and from which f_{micro} the microcanonical averages should be accumulated. We consider a homopolymer consisting of N monomers which may assume any self-avoiding walk (SAW) configuration on a two-dimensional lattice.

Assuming that the polymer is in a bad solvent, there is an effective monomer-monomer attraction in addition to the self-avoidance constraint representing excluded volume. For every pair of nonbonded nearest-neighbor monomers, the energy of the polymer is reduced by ε. The Hamiltonian for the model can be written as

$$\mathcal{H} = -\varepsilon \sum_{\langle i,j \rangle} \sigma_i \sigma_j, \tag{9}$$

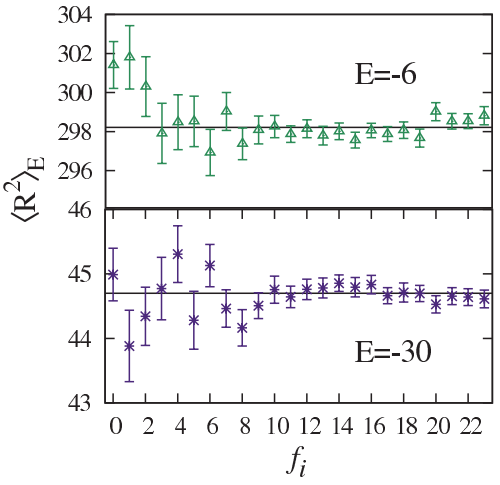

FIG. 14. (Color online) Evolution of the microcanonical average of the mean-square end-to-end distance for $N = 50$ at $E = -6$ and -30 during the simulations over 100 independent runs for each flatness stage.

where $\sigma = 1$ (0) if the site i is occupied (vacant), and the sum is over nearest-neighbor pairs [21]. (The sum is understood to exclude pairs of bonded segments along the chain.) We used the so-called reptation or *"slithering snake"* move, which consists of randomly adding a monomer from one end of the chain and removing a monomer from the other end, maintaining the size of the polymer constant. We define one Monte Carlo step as N attempted moves.

In this model, besides the energy, another quantity of interest is the mean-square end-to-end distance given by

$$\langle R^2 \rangle = \langle [(x_N - x_0)^2 + (y_N - y_0)^2] \rangle. \qquad (10)$$

As prescribed in Sec. II, we updated the density of states and the histogram only after each Monte Carlo step. In order to define from which modification factor to begin accumulating the microcanonical averages, we estimated $\langle R^2 \rangle_E$ for each f_i during the simulations for several energy levels. In Fig. 14, we show these results for $E = -6$ and -30 (the ground state of the $N = 50$ homopolymer is $E_{\min} = -36$). One can see that the microcanonical averages should be accumulated from $f_{\text{micro}} = f_{10}$. On the other hand, to estimate f_{final} for halting the simulations, we calculated the canonical average of the energy and the mean-square end-to-end distance during the simulations for five fixed temperatures, namely, $T = 0.5$, 1.5, 2.5, 3.5, and 4.5. In Fig. 15, we show the behavior of the energy at $T = 1.5$, and in Fig. 16 we show the behavior of the mean-square end-to-end distance at $T = 4.5$. All the graphs we have constructed for these quantities for the temperatures mentioned above have a similar performance. We see, therefore, that for this model the simulations should be carried out up to $f_{\text{final}} = f_{18}$.

Other more elaborate models, such as the HP model of protein folding [22] or continuous (off-lattice) models of polymers [23,24], will require a test similar to the one made in this section that may point to different values for f_{micro} and f_{final}. Notwithstanding that, our results suggest that this final modification factor will occur far before $f_{26} \approx 1 + 10^{-8}$, leading to considerable CPU time savings.

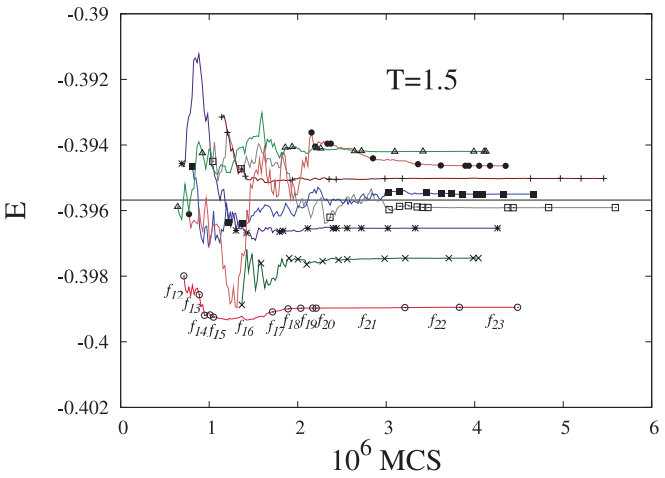

FIG. 15. (Color online) Evolution of the energy at $T = 1.5$ during the WLS for eight independent runs beginning from f_{12}. The straight line is the mean value obtained from 100 independent runs.

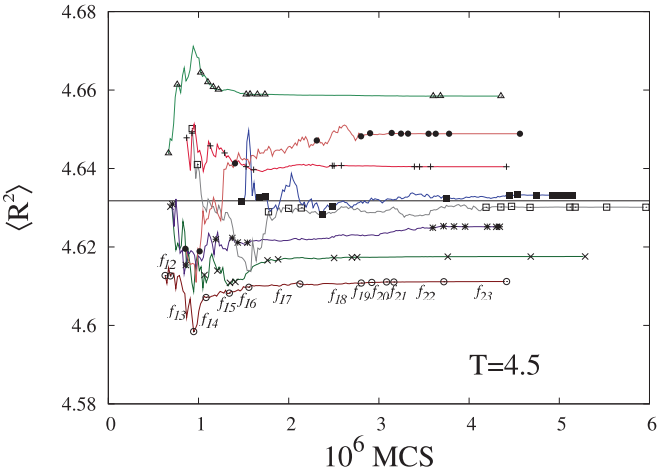

FIG. 16. (Color online) Evolution of the mean-square end-to-end distance at $T = 4.5$ during the WLS for eight independent runs beginning from f_{12}. The straight line is the mean value obtained from 100 independent runs.

VI. CONCLUSIONS

We have demonstrated that the conventional WLS presents problems of accuracy. However, with very few changes in the implementation of the method—namely, updating the density of states only after each Monte Carlo step, halting the simulations for $\ln f < \ln f_{\text{final}}$, with f_{final} determined by the canonical averages during the simulations, and accumulating the microcanonical averages only for $\ln f < \ln f_{\text{micro}}$, where f_{micro} is found from the behavior of the microcanonical averages in each modification factor—it becomes quite accurate. Adopting the Monte Carlo step to update the density of states and delaying the start of the microcanonical averaging are changes that lead to an improved accuracy of the algorithm, while the proper definition of when to stop the simulation (f_{final}) saves a lot of CPU time.

It should be pointed out that a direct comparison of the density of states with exact calculations, although pictorially very impressive, is not a good test for algorithms that estimate the density of states. The canonical and microcanonical averages during the simulations are a more adequate checking parameter for convergence. Another important conclusion is that no single simulation in particular tends to the exact value. One can obtain results as close as possible to the exact value by increasing the number of independent runs.

The great advantage of our findings is that all existing codes using WLS can be promptly adapted to this new procedure just adding a few lines to the computer program.

ACKNOWLEDGMENTS

This work was supported by the Brazilian agencies CNPq and FUNAPE-UFG. We thank Salviano de Araújo Leão for his helpful and substantial advice and support with the computations.

[1] F. Wang and D. P. Landau, Phys. Rev. Lett. **86**, 2050 (2001).
[2] F. Wang and D. P. Landau, Phys. Rev. E **64**, 056101 (2001).
[3] C. Zhou and J. Su, Phys. Rev. E **78**, 046705 (2008).
[4] R. E. Belardinelli and V. D. Pereyra, Phys. Rev. E **75**, 046701 (2007).
[5] R. E. Belardinelli, S. Manzi, and V. D. Pereyra, Phys. Rev. E **78**, 067701 (2008).
[6] R. E. Belardinelli and V. D. Pereyra, J. Chem. Phys. **127**, 184105 (2007).
[7] P. Dayal, S. Trebst, S. Wessel, D. Wurtz, M. Troyer, S. Sabhapandit, and S. N. Coppersmith, Phys. Rev. Lett. **92**, 097201 (2004).
[8] C. Zhou and R. N. Bhatt, Phys. Rev. E **72**, 025701(R) (2005).
[9] See, e.g., M. Plichske and B. Bergersen, *Equilibrium Statistical Physics* (Cambridge University Press, Cambridge, 2008).
[10] A. D. Swetnam and M. P. Allen, J. Comput. Chem. **32**(5), 816 (2011).
[11] P. D. Beale, Phys. Rev. Lett. **76**, 78 (1996).
[12] A Monte Carlo sweep consists of L^2 spin-flip trials.
[13] The study performed in [14] was carried out updating the density of states after every L^2 trial move. Thanks to a fortunate misunderstanding, the authors have adopted the Monte Carlo sweep in analogy with the METROPOLIS algorithm.
[14] C. J. Silva, A. A. Caparica, and J. A. Plascak, Phys. Rev. E **73**, 036702 (2006).
[15] M. E. Fisher, in *Critical Phenomena*, edited by M. S. Green (Academic, New York, 1971).
[16] M. E. Fisher and M. N. Barber, Phys. Rev. Lett. **28**, 1516 (1972).
[17] *Phase Transitions and Critical Phenomena*, edited by C. Domb and J. L. Lebowitz, Vol. 8 (Academic, New York, 1974).
[18] C. J. Silva, A. G. Cunha-Netto, A. A. Caparica, and R. Dickman, Braz. J. Phys. **36**, 619 (2006).
[19] A. G. Cunha-Netto, R. Dickman, and A. A. Caparica, Comput. Phys. Commun. **180**, 583 (2009).
[20] D. T. Seaton, T. Wüst, and D. P. Landau, Phys. Rev. E **81**, 011802 (2010).
[21] R. Dickman, J. Chem. Phys. **96**, 1516 (1992).
[22] T. Wüst and D. P. Landau, Comput. Phys. Commun. **179**, 124 (2008).
[23] T. Wüst and D. P. Landau, Phys. Rev. Lett. **102**, 178101 (2009).
[24] M. P. Taylor, W. Paul, and K. Binder, J. Chem. Phys. **131**, 114907 (2009).